

## ALMA ACA Observations of Molecular Gas in TNT Isolated Pairs

SWETHA SANKAR <sup>1</sup> AND GEORGE C. PRIVON<sup>2</sup>

<sup>1</sup>*University of California, Los Angeles  
405 Hilgard Ave.*

*Los Angeles, CA 90095, USA*

<sup>2</sup>*National Radio Astronomy Observatory, Charlottesville  
520 Edgemont Road  
Charlottesville, VA 22903, USA*

### ABSTRACT

Previous probing via the Sloan Digital Sky Survey (SDSS) spectral energy density distributions (SEDs) confirms enhanced star formation rates for isolated dwarf galaxy pairs with separation distances  $R_{sep} < \sim 100$  kpc. It is however unclear whether these enhancements result from larger molecular gas fractions or an increased efficiency in which these galaxies convert H<sub>2</sub> into stars. From the TiNY Titans survey, we quantify molecular gas reservoirs of a subset of 10 isolated, low redshift dwarf galaxy pairs with short separation distances ( $6 \text{ kpc} < R_{sep} < 48 \text{ kpc}$ ) via dust continuum and CO (2→1) tracers. We successfully detect CO in four galaxies within the data set. With the application of both metallicity dependent and Milky Way accepted  $\alpha_{CO} = 4.3 M_{\odot} (K \text{ km s}^{-1} \text{ pc}^2)^{-1}$  and gas-to-dust ratio (GDR) = 100, we estimate molecular gas masses of  $\sim 10^8 M_{\odot}$ . Similarly, we constrain  $3\sigma$  upper limits for the rest of the galaxies within our data to span  $10^6 - 10^8 M_{\odot}$ .

### 1. INTRODUCTION

Primordial galaxy morphology, whose evolution is a staple to understanding the dynamics responsible for present-day galaxy environments, is still an active topic of debate, often limited by unresolved systems at high red shifts ( $z > 2$ ) (e.g. Yajima et al. 2009; Elmegreen et al. 2008; Melia 2014). An alternative method involves using dwarf galaxies as quintessential tools to probe this inquiry given their structural similarity to primitive galaxies as low-mass, gas-rich, metal-poor environments with baryonic mass dominated by HI gas fractions of 40 - 90% (Stierwalt et al. 2015) and lack of stabilizing features. As such, star formation in low mass dwarfs largely occurs and is modified under different conditions in comparison to more massive galaxies.

Bundy et al. (2015); Blanton et al. (2017); collaboration et al. (2020) have catalogued star formation rates (SFR) in sets of dwarf galaxies in varying stages of interaction via the photoionization of young stars, with a serendipitous result observed in Stierwalt et al. (2015) of significant star formation rate enhancements in low red shift isolated dwarf galaxy pairs with a separation distance of  $R_{sep} < \sim 100$  kpc.

The same pattern observed in more massive interacting galaxies is attributed to gas infall/ outflows to individual galaxy centers driven gravitational influences, accelerating stellar formation (e.g. Cox et al. 2006). For

dwarf galaxies with lower potential wells, however, this explanation is less effective in solely characterizing the detected star formation rate enhancement, suggesting other dynamical processes at play.

The Kennicutt-Schmidt relation  $\Sigma_{SFR} = A \Sigma_{gas}^N$  (Kennicutt Jr 1998) shows a positive correlation between the star formation rate surface density and the integrated molecular gas content within these low-mass systems and offers a mode of quantifying the efficiency in which these galaxies form stars. However it is unclear whether star formation rate enhancements in these systems are a result of higher H<sub>2</sub> content or an increased efficiency in which this gas is converted into stars because their molecular gas masses are unknown.

In this paper, we present new radio interferometric analyses using ALMA Atacama Compact Array (ACA) data taken from the TiNY Titans Survey (TNT) (Stierwalt et al. 2015) to characterize the efficiency of stellar formation in dwarf galaxy pairs. Section (2) discusses ALMA ACA setup/ reimaging, while Sections (3) and (5) detail our approach to calculating molecular gas fractions for these unresolved systems and analyze our measured data. Section (6) evaluates our results in the larger context of low mass galaxy evolution and outlines future applications of this study.

### 2. RADIO INTERFEROMETRY

**Table 1.** Observation Log

Pair Name	DM ID	$R_{sep}$	$z$	$Z^a$	H $\alpha$ EQW	SFR $_{tot}$	HI	
	$M_*$	(kpc)			( $\mu\text{m}$ )	( $M_\odot \text{ yr}^{-1}$ )	( $M_\odot$ )	( $M_\odot$ )
dm0027+00	I097	44	0.0307	8.4	25.63	0.41	$10^{9.5}$	$10^{8.62}$
	I098		0.0311	8.9	41.20	1.33		$10^{9.27}$
dm0035-10	I015	12	0.0372	8.6	35.20	2.00	$10^{9.4}$	$10^{9.13}$
	I016		0.0377	8.4	33.01	0.99		$10^{8.63}$
dm0052+00	I115	48	0.0341	8.7	115.33	5.13	...	$10^{9.33}$
	I116		0.0346	8.9	13.86	1.32		$10^{9.46}$
dm0346+00	I109	47	0.0303	8.9	21.05	0.09	...	$10^{9.28}$
	I110		0.0309	8.5	27.24	0.06		$10^{8.85}$
dm0916+06	I039	18	0.0117	...	32.21	0.13	$10^{9.8}$	$10^{7.83}$
	I040		0.0123	8.5	11.35	0.48		$10^{8.86}$
dm1049+09	I103	45	0.0336	8.6	69.71	0.44	$10^{10.0}$	$10^{9.11}$
	I104		0.0335	8.8	56.34	0.65		$10^{9.34}$
dm1106+01	I095	43	0.0307	8.8	28.93	0.75	$10^{9.6}$	$10^{8.90}$
	I096		0.0312	8.4	64.56	1.90		$10^{8.78}$
dm1152+07	I009	6	0.0317	...	6.25	0.02	$10^{9.3}$	$10^{8.53}$
	I010		0.0315	8.3	255.39	0.62		$10^{8.46}$
dm1231+06	I079	37	0.0306	8.3	51.48	0.15	$10^{9.5}$	$10^{8.11}$
	I080		0.0305	8.2	53.34	0.06		$10^{8.27}$
dm2227-09	I071	31	0.0055	...	14.22	0.11	$10^{9.4}$	$10^{7.90}$
	I072		0.0057	8.0	137.02	0.32		$10^{7.74}$

<sup>a</sup>Certain parameters are omitted due to low SNR in SDSS observations.

Radio interferometric data were obtained via ALMA ACA 7m array Band 6 ( $\sim 6''$ ) observations of low-redshift dwarf galaxy pairs selected from the TiNy Titans Survey (Stierwalt et al. 2015), with the exclusion of objects at  $\delta > +10^\circ$  and redshifts  $z > 0.04$  to avoid shadowing of antennas and insensitivity to cold dust emission respectively. No additional cuts based on the intrinsic properties of these systems are made to ensure an unbiased investigation. The data set is composed of galaxy pairs spanning masses of  $10^7 M_\odot < M < 10^{9.7} M_\odot$ , separation distances of  $6 \text{ kpc} < R_{sep} < 48 \text{ kpc}$ , star formation rates of  $0.06 - 2.39 M_\odot \text{ yr}^{-1}$ , and oxygen abundant metallicities of  $Z = 8.0 - 8.9$  with a median of  $Z = 8.6$ . The tuning was set to cover the observed frequencies of the H<sub>2</sub> gas tracers CO (2 $\rightarrow$ 1) and CS (5 $\rightarrow$ 4) within these redshifts. Table (1) references parameters previously observed by SDSS of these TNT dwarf pairs.

The RMS continuum emission is constrained to a  $3\sigma$  detection threshold of  $M_{dust} = 5 \times 10^6 M_\odot$  set from Rémy-Ruyer et al. (2015) assuming  $\beta = 1.8$  and  $T_{dust} = 25 \text{ K}$ . Within this limit, we are sensitive to  $L'_{CO(2\rightarrow 1)} = 5 \times 10^7 \text{ K km s}^{-1} \text{ pc}^2$  for a  $50 \text{ km s}^{-1}$  line, corresponding to a H<sub>2</sub> mass of  $M_{H_2} > 2.4 \times 10^8 M_\odot$  for an  $\alpha_{CO} > 4.8 M_\odot$ .

Each source is targeted with two pointings with the exception of dm0035-10 and dm1152+07 which fit within a single ACA 7 m primary beam.

### 3. ANALYSIS

Cold H<sub>2</sub> is invisible in emission due to a lack of dipolar rotational transitions given its molecular structure and only warm H<sub>2</sub> is observable in the mid and near infrared. Thus, alternative, complementary agents are often used to indirectly track the molecular gas quantity.

A common tracer identified in literature is CO (1 $\rightarrow$ 0), which is related to H<sub>2</sub> mass via a metallicity dependent and empirically determined scaling factor  $\alpha_{CO}$ . As we are searching for CO (2 $\rightarrow$ 1), we relate CO (1 $\rightarrow$ 0) and CO (2 $\rightarrow$ 1) via a fixed line ratio  $R_{21} = 0.8$  before the application of the scaling factor, which is  $4.3 M_\odot (\text{K km s}^{-1} \text{ pc}^2)^{-1}$  for the Milky Way (Bolatto et al. 2013) with an uncertainty  $\pm 30\%$ . Eqn (1) provides this relation:

$$M_{H_2, CO} = \alpha_{CO} R_{21} L_{CO} \quad (1)$$

Here,  $L_{CO} = 2453 S_{CO} \Delta v D_L^2 / (1+z)$ , where  $S_{CO} \Delta v$  is the integrated line flux density in  $\text{Jy km/s}$ ,  $D_L$  is the luminosity distance in  $\text{Mpc}$ , and  $z$  is the galaxy's redshift.

We additionally approach calculations via the cold dust continuum emission, related to H2 content via a metallicity dependent GDR taken from Rémy-Ruyer et al. (2014).

$$M_{H2,dust} = \frac{L_\nu}{4\pi B_\nu(T_{dust})\kappa_\nu} \frac{G}{D} \quad (2)$$

In Eqn (2),  $L_\nu = F4\pi D_L^2/(1+z)^3$  in  $W/Hz$ , where  $F$  is set by the continuum RMS,  $\kappa_\nu$  is set to be  $\beta = 1.8$  by Abergel et al. (2011), and  $B_\nu(T_{dust})$  refers to the blackbody radiation at  $T_{dust} = 25 K$ .

#### 4. DATA REDUCTION

ALMA ACA data is reduced using the Common Astronomy Software Application (CASA) (McMullin et al. 2007). Per galaxy, we first image the dirty cube to identify any CO emission. Continuum subtraction is not performed beforehand as line-free channels in the visibility data reflect the noise. We then proceed to image this data using the task TCLEAN to create a cleaned cube image using a threshold set to  $0.5\sigma$  the RMS value of the corresponding dirty cube using natural weighting, Hogbom deconvolution, and a large value for maximum iterations. TCLEAN is run once again under the same conditions to create a multi frequency synthesis (mfs) image representing cold dust emission per galaxy with the exclusion of channels where we expect CO emission to lay.

Per cleaned cube, we ascertain a CO integrated line flux density via a moment 0 map created. We first identify the spatial region of the emission from the moment map, extract a spectrum from the cube using this region, and apply the task SPECFLUX to the channels containing the emission determined by the spectrum. The pipeline produced value is compared when necessary. For galaxies where we do not detect CO emission, we use the largest line width from identified detections and multiply by  $3\sigma$  of the cube cleaned RMS to place an upper limit on H2 mass.

The continuum image RMS sets continuum upper limits on dust mass per galaxy and is later converted to a molecular gas mass with the application of a metallicity dependent GDR taken from Rémy-Ruyer et al. (2014). Table (2) lists each measured quantity, later converted to a molecular gas mass.

#### 5. RESULTS

For the first time, ACA observations of isolated dwarf galaxy pairs have revealed the presence of the CO (2→1) tracer in four dwarf galaxies: dm0027+00 I098, dm1049+09 I104, dm0052+00 I115, and dm0346+00 I109. These systems have higher metallicities within

our data set, suggesting larger fraction of CO present for a fixed H2 mass, possibly explaining why CO was only detectable in these systems.

Tables (2) and (3) lists upper limit continuum flux and upper limit/ detected CO flux density measurements from which the molecular gas masses of these galaxy pairs are determined. We compare H2 masses from the application of a metal dependent  $\alpha_{CO}$  and GDR and the canonically accepted Milky Way values of  $\alpha_{CO} = 4.3 M_\odot$  and  $GDR = 100$ . For galaxies in which we have CO detections, we determine molecular gas masses to be approximately  $10^8 M_\odot$ , while placing upper limits for the rest of our data set, varying from  $10^6 - 10^8 M_\odot$ . As our data set is largely unresolved, we are unable to glean additional information of velocity fields and dispersion.

Figure (1) checks the uniformity of our resulting mass calculations via the two alternative methods we employ. We conclude calculations to overall be broadly consistent.

An additional analysis of the H2/HI mass fraction of all isolated pairs (bar dm0052+00 and dm0346+00 for which we do not have HI mass values) is depicted in figure (2). We examine gas phase as a function of the following properties: averaged metallicity, separation distance, and averaged stellar mass. While we expect closer separations to result in higher H2 gas fractions produced by more HI-H2 conversions aided by interactions of the HI envelopes of the primary and secondary galaxy within the pair, we instead find less than 30% of the gas within these galaxies to be molecular, smaller than the HI gas fraction of 40 – 90% for our pairs.

In figure (3), we compare the star formation/molecular gas relation of our galaxies to galaxies in the local group via the XCOLD GASS IRAM 30 m survey (Saintonge et al. 2017) spanning a stellar mass range of  $10^9 - 10^{11.5}$ , overlapping with the upper mass end of our data set. In this context, the galaxies within the TNT data set have lower H2 content and star formation rates.

#### 6. CONCLUSION AND DISCUSSION

We present analyses of a set of ten, low redshift, TiNy Titans isolated dwarf galaxy pairs with SDSS observed star formation rate enhancement. In quantifying H2 masses for these sources to determine forces driving these increased star formation rates, we investigate CO (2→1) and cold dust tracers for our 20 sources. Our main observations are as follows:

1. CO (2→1) is detected in four of our more metal-rich sources - dm0027+00 I098, dm1049+09 I104, dm0052+00 I115, and dm0346+00 I109 for which we calculate H2 masses within  $10^8 M_\odot$ .

**Table 2.** Measured Quantities

Pair Name	DM ID	CO(2→1) Flux Density ( $Jy km s^{-1}$ )	Continuum Flux (mJy)
dm0027+00	I097	<1.54	<0.408
	I098	1.71	<0.451
dm0035-10	I015	<1.16	<0.480
	I016	<1.71	<0.390
dm0052+00	I115	1.46	<0.574
	I116	<2.62	<0.550
dm0346+00	I109	2.28	<0.634
	I110	<3.01	<0.653
dm0916+06	I039	<3.78	<0.819
	I040	<3.67	<0.614
dm1049+09	I103	<2.30	<0.621
	I104	3.53	<0.645
dm1106+01	I095	<3.65	<0.468
	I096	<3.43	<0.489
dm1152+07	I009	<1.41	<0.531
	I010	<2.40	<0.527
dm1231+06	I079	<2.85	<0.614
	I080	<2.82	<0.620
dm2227-09	I071	<1.05	<0.268
	I072	<1.84	<0.193

- For CO absent systems, we place  $3\sigma$  upper limits via cold dust continuum emission and approximated CO flux densities, resulting in molecular gas limits ranging from  $10^6 - 10^8 M_{\odot}$
- Within limits, less than 30% of the gas in each galaxy pair is molecular.
- Star formation rates and molecular gas masses of the TNT data is consistent with the XCOLD GASS local galaxies within the errors, with the TNT data having lower values given their lower stellar masses.

## 7. FUTURE WORK

While quantifying molecular gas reservoirs allows us to draw conclusions with regards to the fraction of stars enriched in these systems, future extension of this work includes an investigation of alternative parameters influencing stellar evolution, including but not limited to: AGNs, tidal tails, etc. We propose future high resolution work to delineate areas of molecular gas and active star formation with these TNT pairs to identify alternative dynamical processes driving up star formation rates. Additionally, future work will include longer observation blocks to detect CO.

## REFERENCES

- Abergel, A., Ade, P. A., Aghanim, N., et al. 2011, *Astronomy & Astrophysics*, 536, A25
- Blanton, M. R., Bershadsky, M. A., Abolfathi, B., et al. 2017, *AJ*, 154, 28, doi: [10.3847/1538-3881/aa7567](https://doi.org/10.3847/1538-3881/aa7567)
- Bolatto, A. D., Wolfire, M., & Leroy, A. K. 2013, *Annual Review of Astronomy and Astrophysics*, 51, 207
- Bundy, K., Bershadsky, M. A., Law, D. R., et al. 2015, *ApJ*, 798, 7, doi: [10.1088/0004-637X/798/1/7](https://doi.org/10.1088/0004-637X/798/1/7)
- collaboration, S.-I., et al. 2020, *Astrophys. J. Suppl*, 249
- Cox, T., Di Matteo, T., Hernquist, L., et al. 2006, *The Astrophysical Journal*, 643, 692
- Elmegreen, B. G., Bournaud, F., & Elmegreen, D. M. 2008, *The Astrophysical Journal*, 688, 67
- Kennicutt Jr, R. C. 1998, *The Astrophysical Journal*, 498, 541
- McMullin, J. P., Waters, B., Schiebel, D., Young, W., & Golap, K. 2007, 376, 127
- Melia, F. 2014, *The Astronomical Journal*, 147, 120

**Table 3.** Derived Quantities

Pair Name	DM ID	$L'_{CO}$ ( $10^6 K km s^{-1} pc^2$ )	$M_{H2,CO\sim X}$ ( $10^6 M_{\odot}$ )	$M_{H2,CO\sim MW}$ ( $10^6 M_{\odot}$ )	$L_{dust}$ ( $10^{19} W/Hz$ )	$M_{H2,GDR\sim X}$ ( $10^6 M_{\odot}$ )	$M_{H2,GDR\sim 100}$ ( $10^6 M_{\odot}$ )
dm0027+00	I097	<83	<266	<286	<243	<172	<172
	I098	137	437	470	<278	<197	<197
dm0035-10	I015	<99	<316	<340	<140	<91	<91
	I016	<113	<362	<389	<117	<151	<76
dm0052+00	I115	66	253	271	<141	<148	<93
	I116	<110	<466	<501	<139	<116	<92
dm0346+00	I109	97	310	333	<124	<80	<80
	I110	<133	<426	<456	<133	<171	<86
dm0916+06	I039	<24	...	<82	<19	...	<12
	I040	<25	<81	<88	<21	<44	<14
dm1049+09	I103	<120	<385	<414	<89	<125	<63
	I104	184	588	632	<115	<128	<81
dm1106+01	I095	<158	<506	<544	<93	<104	<66
	I096	<154	<495	<532	<101	<143	<72
dm1152+07	I009	<66	...	<226	<113	...	<74
	I010	<110	<353	<380	<111	<362	<72
dm1231+06	I079	<124	<395	<425	<167	<398	<80
	I080	<121	<389	<418	<123	<503	<80
dm2227-09	I071	<1	...	<5	<2	...	<1
	I072	<3	<11	<9	<1	<7	<1

the above table, upper limits distinguish systems which lack CO detections.

Rémy-Ruyer, A., Madden, S., Galliano, F., et al. 2014, *Astronomy & Astrophysics*, 563, A31  
—, 2015, *Astronomy & Astrophysics*, 582, A121  
Saintonge, A., Catinella, B., Tacconi, L. J., et al. 2017, *The Astrophysical Journal Supplement Series*, 233, 22  
Stierwalt, S., Besla, G., Patton, D., et al. 2015, *The Astrophysical Journal*, 805, 2

Yajima, H., Umemura, M., Mori, M., & Nakamoto, T. 2009, *Monthly Notices of the Royal Astronomical Society*, 398, 715

In

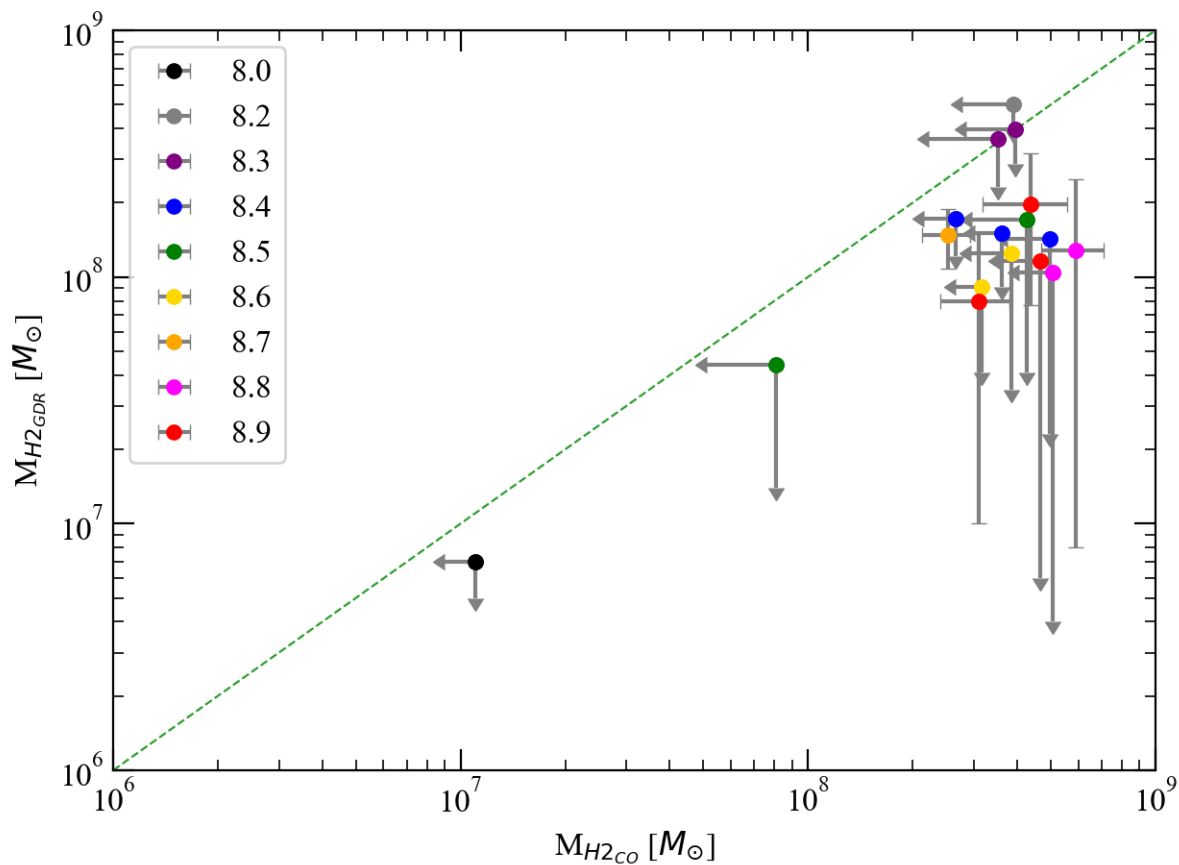


**Figure 1.** The above figure compares the consistency of molecular gas calculations from CO and dust continuum tracers with metallicities color-coded to identify over/underestimations of gas mass. The dotted line represents a 1:1 ratio. Overall, calculations are broadly consistent.

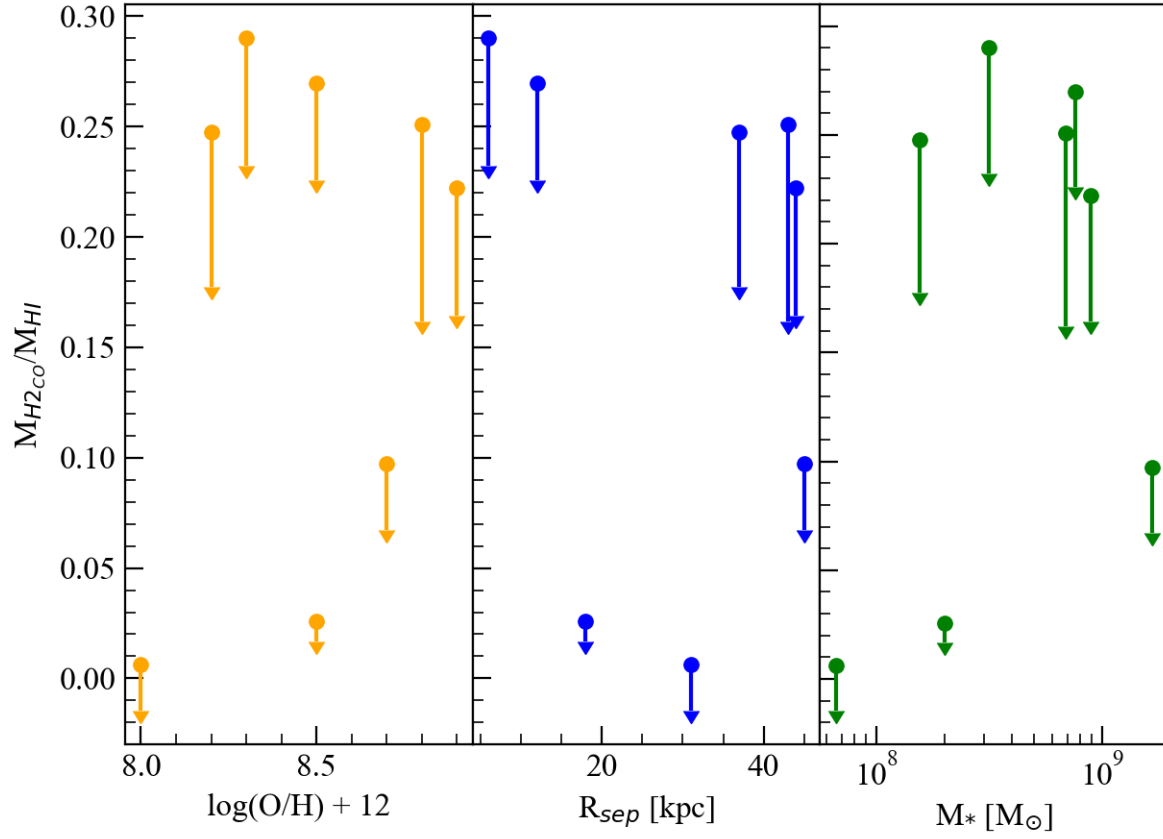


**Figure 2.** We analyze gas phase as a function of metallicity, separation distance, and stellar mass of the TNT galaxy pairs for which we additionally have HI observations. Within limits, we determine less than 30% of the gas in each galaxy to be molecular.

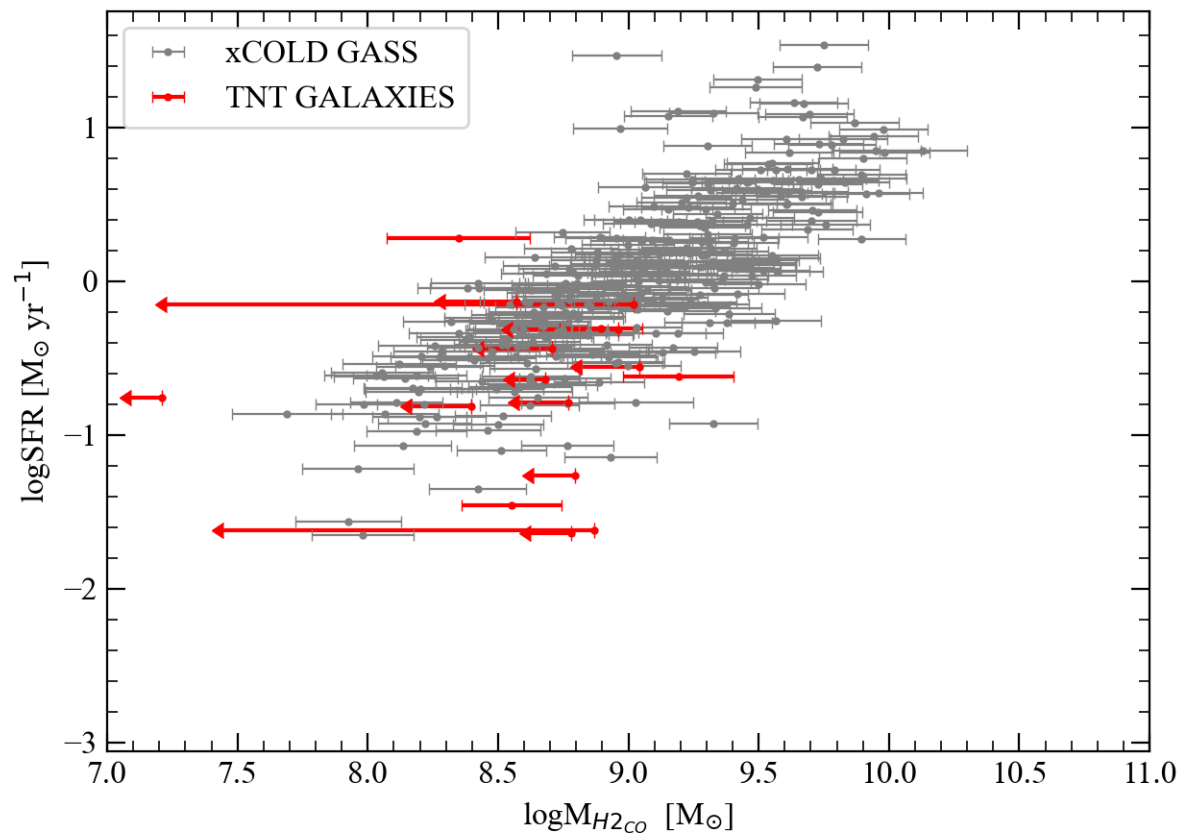


**Figure 3.** We compare molecular gas mass vs star formation rate relation for each individual TNT galaxy to the xCOLD GASS survey sample consisting of larger masses representative of the local galaxy population. As expected, the TNT galaxies have lower gas masses and star formation rate.